


Double-Network Hydrogels Including Enzymatically Crosslinked Poly-(2-alkyl-2-oxazoline)s for 3D Bioprinting of Cartilage-Engineering Constructs.

Journal Article

Author(s):

Trachsel, Lucca; Johnbosco, Castro; Lang, Thamar; Benetti, Edmond M.; [Zenobi-Wong, Marcy](#) 

Publication date:

2019-12-09

Permanent link:

<https://doi.org/10.3929/ethz-b-000381607>

Rights / license:

[In Copyright - Non-Commercial Use Permitted](#)

Originally published in:

Biomacromolecules 20(12), <https://doi.org/10.1021/acs.biomac.9b01266>

Funding acknowledgement:

166052 - Chondrogenic Biopinks for Bioprinting Stable Cartilage Grafts (SNF)

Double-Network Hydrogels Including Enzymatically Crosslinked Poly-(2-alkyl-2-oxazoline)s for 3D Bioprinting of Cartilage Engineering Constructs

*Lucca Trachsel^{a,d}, Castro Johnbosco^{a,d}, Thamar Lang^a, Marcy Zenobi-Wong^{*a},
Edmondo Benetti^{*b,c}*

^aTissue Engineering + Biofabrication Laboratory, Department of Health Sciences and
Technology, ETH Zürich, Zürich, Switzerland.

E-mail: marcy.zenobi@hest.ethz.ch; Tel: +41 44 632 50 89

^b Laboratory for Surface Science and Technology,
Department of Materials, ETH Zürich, Zürich, Switzerland.

^c Biointerfaces, Swiss Federal Laboratories for Materials Science and Technology (Empa),
Lerchenfeldstrasse 5, CH-9014, St. Gallen, Switzerland

E-mail: edmondo.benetti@mat.ethz.ch; Tel: +41 44 632 60 50

^d These authors equally contributed to this work.

KEYWORDS: double-network hydrogels; poly(2-oxazoline); 3D printing; enzymatic crosslinking; Sortase A

Abstract

Double-network (DN) hydrogels are fabricated from poly(2-ethyl-2-oxazoline) (PEOXA)-peptide conjugates, which can be enzymatically crosslinked in the presence of Sortase A (SA), and physical networks of alginate (Alg), yielding matrices with improved mechanical properties with respect to the corresponding PEOXA and Alg single networks, and excellent biocompatibility towards encapsulated human auricular chondrocytes (hACs). The addition of a low content of cellulose nanofibrils (CNF) within DN hydrogel formulations provides to these the rheological properties that ensure their subsequent extrusion-based 3D printing, generating constructs with good shape fidelity. In the presence of hACs, PEOXA-Alg-CNF pre-hydrogel mixtures can be bioprinted, finally generating 3D structured DN hydrogel supports showing cell viability > 90%. Enlarging the application of poly(2-alkyl-2-oxazoline) (PAOXA)-based formulations in the designing of tissue engineering constructs, this study further demonstrates how SA-mediated enzymatic crosslinking represents a suitable and fully orthogonal method to generate biocompatible hydrogels with fast kinetics.

Introduction

Synthetic hydrogels represent a widespread platform for the fabrication of tissue engineering constructs, and in addition, they are extremely versatile supports for studying cellular behavior in the three dimensions (3D).¹⁻⁴ The application of synthetic polymers in hydrogel formulations ensures a full control over the molecular weight, topology and chemical functionality of the components of the network, and enables an extremely broad tuning potential for physicochemical properties that are of relevance in the designing of biomaterials, including chemical composition, degradability, and mechanical properties.⁵ Despite these attractive properties, most of synthetic hydrogels that are formed through covalent crosslinks are characterized by “static” properties, which cannot recapitulate the dynamic nature of the native extracellular matrix (ECM).⁶⁻⁹ Hence, hydrogels exhibiting time-dependent properties, which better match natural physiological environments have been progressively introduced.¹⁰ These encompassed synthetic polymer components that undergo proteolytic¹¹ or hydrolytic¹² degradation, stress-relaxation¹³ or reversibly crosslinking moieties.^{14,15} Besides matrices built up from a single polymeric component, hydrogels featuring broadly tunable and dynamic properties were obtained through the formation of double networks (DN), where two differently crosslinked polymers are intimately mixed. One of the two networks is typically densely and covalently crosslinked, while a secondary network is infused in the former, and includes sparsely and non-covalently crosslinked functions.^{16,17} Usually, the primary, covalently crosslinked network provides elasticity but suffers from brittleness, whereas the secondary, non-covalently crosslinked network provides reversibility and ductility to the entire material.¹⁸ The resulting interpenetrating DN result in a mechanically reinforced matrix with improved strength and toughness, which is mainly due to strong network entanglement¹⁹ and the large strain hysteresis effect.²⁰

In this work, we develop a DN hydrogel based on enzymatically crosslinked poly(2-alkyl-2-oxazoline) (PAOXA) coupled to alginate, which is crosslinked through ionic interactions. Within the obtained matrix human articular chondrocytes can be encapsulated with excellent viability, and the DN formulation can be further used as bioink to fabricate 3D structured, cell-loaded scaffolds by extrusion-based rapid prototyping.

The choice of PAOXA as component of the DN is particularly strategic, since this polymer class has been increasingly applied in a variety of formulations for biomaterials and medical devices, and PAOXAs are progressively emerging as biocompatible and chemically versatile alternatives to poly(ethylene glycol) (PEG) and its derivatives.^{44, 53–55, 45–52}

Random copolymers featuring poly(2-ethyl-2-oxazoline) (PEOXA) with 15 mol% of pendant peptide units were synthesized by cationic ring opening polymerization (CROP) followed by post functionalization, and subsequently applied as precursors for the formation of the covalent network, which was obtained by enzymatic crosslinking in the presence of transpeptidase Sortase A (SA). SA covalently reacts proteins with an LPXTG (X = any alpha L-amino acid except L-proline) C-terminal recognition motif to N-terminal oligoglycines (G)_n (n ≥ 3), which are present on cell walls of Gram-positive bacteria.³⁴ In particular, SA cleaves the amide bond between threonine and glycine fragments within LPXTG sequences, and forms a new amide linkage between the amino terminal group of (G)_n and the threonine fragment on the LPXTG recognition motif.³⁵ When applied to polymer-peptide conjugates, this enzymatic reaction generates hydrogels with faster gelation kinetics under physiological conditions^{36–38} with respect to the more commonly used transglutaminase activated factor XIII.^{39–41} In addition, SA-catalyzed crosslinking is characterized by high specificity and bio-orthogonality,⁴² and does not require the presence of strong nucleophiles or electrophiles, such as in the case of Michael addition-based reactions,⁴³ or

UV light and photoinitiators, which show a more pronounced cross-reactivity towards biomolecules and can affect cell viability.^{44,45}

The enzymatically crosslinked PEOXA network was combined with an alginate hydrogel, yielding a DN with a broader tuning potential of mechanical properties and increased cytocompatibility. Ionically crosslinked alginate was previously applied to mechanically reinforce a covalently crosslinked polyacrylamide (PAAm) network, resulting in a DN matrix with increased fracture energy and stretchability.⁴⁶ Addition of cellulose nanofibrils (CNF) to the DN formulation enhances the shear thinning and shear recovery properties of the pre-hydrogel mixture,^{47,48} finally enabling successful 3D printing in the presence of human auricular chondrocytes (hACs). These hydrogel scaffolds were characterized by high shape fidelity and excellent cell viability, highlighting the proposed DN hydrogels as suitable materials for the fabrication of tissue engineering supports, and enlarging the applicability of PAOXAs in the designing of biomaterials.

Experimental Section

Materials

Hydrazine monohydrate, 2-ethyl-2-oxazoline (EOXA), methyl para-toluenesulfonate (MeOTs), 2-chloroethylammonium chloride, sodium sulfate anhydrous, sodium carbonate anhydrous, potassium hydroxide (KOH), 2,2'-(ethylenedioxy)diethanethiol (EDDT), trifluoroacetic acid (TFA), triethanolamine (TEOA), barium oxide, tri(hydroxymethyl)amino methane (TRIS), and (2-hydroxyethyl)-1-piperazineethanesulfonic acid (HEPES) sodium salt were purchased from Sigma Aldrich. Dimethyl 3,3'-dithiodipropionate was purchased from TCI chemicals. Methanol (MeOH), hydrochloric acid (HCl), glacial acetic acid, and triethylamine (TEA) were purchased from Merck Millipore. Dichloromethane (DCM, extra dry), acetonitrile (ACN, extra dry over

molecular sieves), triisopropylsilane (TIPS), and methyl succinyl chloride were purchased from Acros Organics. 2-Morpholinoethanesulfonic acid hydrate (MES hydrate), tris-(2-carboxyethyl)-phosphine hydrochloride (TCEP-HCl), divinyl sulfone (DVS), 1-ethyl-3-(3-(dimethylamino)propyl)carbodiimide hydrochloride (EDC-HCl) and ethyl isonipecotate were purchased from Fluorochem. EOXA and TEA were distilled over KOH under nitrogen prior to use and stored under argon. MeOTs and ethyl isonipecotate were distilled under high vacuum over CaH₂ and stored under argon. All the other chemicals were used as received. Sodium alginate PRONOVA UP-MVG was purchased from NovaMatrix. Cellulose nanofibrils (CNF), (SUPPORTTM) were purchased from (CELLINK, Gothenberg, Sweden). Sortase A (SA) was produced and purified as previously reported by our group.⁴⁹

*3,3'-Dithiobis(propanoic dihydrazide) (DTPHY)*⁵⁰

Dimethyl 3,3'-dithiodipropionate (25g, 104.9 mmol) was dissolved in 400 mL MeOH and hydrazine monohydrate (30.5 mL, 629.4 mmol, 6 equiv) was added dropwise at 0° C during 1 hour, and later on stirred overnight. The reaction mixture was subsequently cooled down with an ice bath and then the solid product was filtered under vacuum, and later on washed with cold methanol (2 x 20mL) and water (20 mL). The white precipitate was recrystallized once in MeOH and subsequently dried under high vacuum, yielding white crystals (21.25 g, 89.2 mmol, 85%).

¹H NMR (400 MHz, D₂O) δ = 9.05 (s, 2H), 4.21 (s, 4H), 2.88 (t, 4H), 2.40 (t, 4H).

¹³C NMR (76 MHz, D₂O) δ = 173.10, 33.06, 33.00. The ¹H NMR and ¹³C NMR spectra are reported in in the Supporting Information in Figure S1 and S2, respectively.

*Methyl-7-chloro-4-oxo-5-azaheptanoate*⁵¹

Methyl succinyl chloride (25.0 g, 166 mmol, 1 eq.) and 2-chloroethylammonium chloride (19.3 g, 166 mmol, 1 eq.) were suspended in dry DCM (200 mL), cooled down to 0 °C with an ice bath, following dropwise addition of TEA (53 mL, 380 mmol, 2.2 eq.) over a period of 1h. The suspension was then allowed to warm to ambient temperature and stirred overnight before water (100 mL) was added. The organic phase was subsequently washed with 1 M HCl, water and brine (each 100 mL) and finally dried over anhydrous sodium sulfate. After filtration and solvent removal, the residual oil was purified on a plug of neutral alumina gel (8 cm) eluting with DCM:MeOH (99:1). The product was obtained as a light yellow oil (26.48 g, 136.8 mmol, 83.3%). ¹H NMR (400 MHz, CDCl₃) δ = 6.33 (s, 1H), 3.65 (s, 3H), 3.61 – 3.49 (m, 4H), 2.64 (t, J = 6.8 Hz, 2H), 2.49 (t, J = 6.7 Hz, 2H). ¹³C NMR (76 MHz, CDCl₃) δ = 173.45, 171.78, 51.94, 43.91, 41.36, 30.89, 29.30 ppm.

*2-methoxycarboxyethyl-2-oxazoline (MestOXA)*⁵¹

Methyl 4-(2-chloroethyl)amino-4-oxobutanoate (26.48 g, 136.8 mmol, 1 eq.) and anhydrous sodium carbonate (11.6 g, 109.4 mmol, 0.8 eq.) were reacted (neat) in a 250 mL round-bottom flask (RBF) mounted on a rotary evaporator (40° C, 20 mbar) for 2 days until the formation of CO₂ stopped, indicating full completion of the reaction. Subsequently, the reaction mixture was dissolved with 100 mL of DCM and the salts were filtered off. After removal of the solvent, the crude product was obtained as a yellow oil that was further purified by distillation from barium oxide under reduced pressure (2.3 x 10⁻² mbar, 92°C), yielding a colorless oil (14.81 g, 94.4 mmol, 69%).

^1H NMR (400 MHz, CDCl_3): δ = 4.24 ppm (t, J = 9.73 Hz, 2 H), 3.82 (t, J = 9.16 Hz, 2 H), 3.70 (s, 3 H), 2.68 (t, J = 7.44 Hz, 2 H), 2.58 (t, J = 7.44 Hz, 2 H); ^{13}C NMR (76 MHz, CDCl_3): δ = 172.8, 167.0, 67.5, 54.4, 51.8, 30.1, 23.1 ppm. The ^1H NMR and ^{13}C NMR spectra are reported in the Supporting Information in Figure S3 and S4, respectively.

PEOXA-COOCH₃

15 mL of dry ACN, EOXA (9.23 g, 93.1 mmol, 170 eq.) and MestOXA (2.58 g, 16.4 mmol, 30 eq.) was added to an oven-dried two-neck RB flask under N_2 . After stirring the reaction mixture for 10 min at 0°C , MeOTs (102 mg, 0.55 mmol, 1 eq.) was added on ice and stirred for another 10 min. Then the reaction mixture was heated to 80°C and stirred for 48 h under argon. After this time, the polymerization was terminated by adding an excess of ethyl isonipecotate (800 μL , 5 mmol, 10 eq.) at room temperature, and left stirring for another 48 h under argon. The solvent was removed under reduced pressure, and the crude polymer dissolved in 100 mL of deionized water and purified by dialysis against ultrapure water using 1 kDa molecular weight cut-off (MWCO) dialysis membranes (Spectra-Por) for two days. The PEOXA-COOCH₃ (9.45 g, 80 % yield) was obtained after lyophilization as a white powder. The chemical structure and the purity of the synthesized polymer were determined by ^1H -NMR (400 MHz) (Figure S5) and the molecular weight measured by gel permeation chromatography (GPC) as reported in the Supporting Information (Table S1).

PEOXA-COOH

The methyl and ethyl ester of the side chains and the end groups of the synthesized PEOXA-COOCH₃ copolymers were hydrolyzed with 1 M NaOH for 24 h at room temperature. Glacial

acetic acid was added until pH 6 was reached before the polymer was purified by dialysis in the same way as before and finally lyophilized to yield a white powder (8.5 g, 90% yield).

PEOXA-VS

In a typical reaction, PEOXA-COOH (2g, n(-COOH) = 2.8 mmol, 1 eq., 15% substitution degree of -COOH) was solubilized in 20 mL MES buffer (150 mM) while the pH of the resulting solution was 4.5. Later on, DTPHY (1.33 g, 5.6 mmol, 2 eq.) and EDC-HCl (1.6 g, 8.4 mmol, 3 eq., predissolved in 5 mL of H₂O) were sequentially added while stirring the solution, and this mixture was left reacting for 4 h. TCEP-HCl (2.4 g, 8.4 mmol, 3 eq.) was subsequently added and the mixture was reacted overnight. The obtained polymer was purified by dialysis against acidified ultrapure water (pH 3) for 2 days, yielding thiolated PEOXA-SH. The purified solution of PEOXA-SH was transferred to a dropping funnel, and later on added dropwise to a DVS solution (16.5 g, 140 mmol, 50 eq.) in 100 mL TEOA (300mM, pH 8.0) buffer, which was previously subjected to N₂ bubbling for 10 min. Following this addition, the mixture was left reacting for 1 h under stirring, and then dialyzed against ultrapure water for 2 days. PEOXA-VS (2.35 g, 75 % yield) was obtained after freeze-drying as a white powder. Chemical identity and purity of PEOXA-VS were determined by ¹H-NMR (400 MHz) (Figure S6).

Peptide synthesis

Peptides were synthesized by Fmoc solid phase-supported synthesis (SPPS), on an automated peptide synthesizer (Prelude, Protein Gyros Technologies) using Rink amide resin. Cleavage of peptides from the resin, and removal of the protecting groups was performed manually using 2.5 % EDDT, 2.5% TIPS, 2.5% H₂O, 92.5% TFA solution. The cleavage was performed for 2 h at

room temperature. The peptides were precipitated in cold diethyl ether twice before purification through preparative RP-HPLC, using C18 column with 50-90% ACN/H₂O linear gradient over 20 min. The purity of the peptides was confirmed by analytical RP-HPLC using an Agilent 1260 infinity equipped with a Poroshell EC-C18, 2.7 μm bead size, and 4.6 x 100 mm column with 10-90% ACN/H₂O linear gradient, while monitoring the absorbance at 214 nm. The identity of the peptides was confirmed by electrospray ionization mass spectroscopy (ESI-MS) using a Water instrument equipped with a single quadrupole detector SQ 2.

LC-MS (ESI-TOF): for GCRELPETGG [M + H]⁺ calculated: 1017.47, found: 1017.8; for GGGGLERCL calculated: 860.43, found: 860.7.

PEOXA-peptide conjugates

PEOXA-GGGG. PEOXA-VS (400 mg, n(-VS) = 0.4 mmol, 1 eq.) was dissolved in 10 mL TEOA buffer (300 mM, pH 8) and the solution was de-oxygenated by N₂ bubbling. Later on, 10 mL solution of GGGGLERCL (M_w 860 g/mol, 520 mg, 0.6 mmol, 1.5 eq.) in H₂O was added dropwise during 30 min under stirring, and left reacting overnight at room temperature under N₂. Finally, the resulting mixture was purified by dialysis against ultrapure water using 3.5 kDa MWCO dialysis membranes for two days. The chemical structure and the purity of the PEOXA-GGGG were determined by ¹H-NMR (400 MHz), as reported in Figure S7.

PEOXA-LPETG. PEOXA-VS (380 mg, n(-VS) = 0.38 mmol, 1 eq.) was dissolved in 10 mL TEOA buffer (300 mM, pH 8), and the mixture was subsequently degassed by N₂ bubbling for 10 min. A 10 mL solution of GCRELPETGG (M_w 1017 g/mol, 580 mg, 0.57 mmol, 1.5 eq.) in H₂O was later on added dropwise during 30 min, and left reacting overnight at room temperature under N₂. After that, the solution was purified by dialysis against ultrapure water employing 3.5 kDa MWCO

dialysis membranes for 2 days. The chemical structure and the purity of the PEOXA-LPETG were determined by $^1\text{H-NMR}$ (400 MHz), as reported in Figure S8.

NMR Spectroscopy

^1H NMR spectra were recorded on a Bruker Avance DRX-400 at room temperature, using CDCl_3 and D_2O as solvents.

Size Exclusion Chromatography (SEC)

An Agilent 1100 GPC/SEC unit was used equipped with two PFG linear M columns (PSS) connected in series with an Agilent 1100 VWD/UV detector operated at 230 nm, as well as a DAWN HELEOS 8 multi-angle laser light scattering (MALS) detector followed by an Optilab T-rEX RI detector, both from Wyatt. Samples were eluted in hexafluoroisopropanol (HFIP) with 0.02 M K-TFAc at 1 mL min^{-1} at room temperature. Absolute molecular weights were evaluated with Wyatt ASTRA software and dn/dc values based on our analytical setup ($\text{dn/dc}_{\text{PEOXA}} = 0.2283 \text{ mL g}^{-1}$).

Hydrogel Preparation

PEOXA-based single networks were prepared by dissolving PEOXA-peptide conjugates (PEOXA-LPETG and PEOXA-GGGG) in Tris buffered saline (TBS, 50 mM of Tris, 150 mM of NaCl, adjusted to $\text{pH} = 7.4$), obtaining polymer solution with 5% (w/v) of PEOXA-LPETG and PEOXA-GGGG. After addition of $10 \mu\text{M}$ SA, covalent networks of PEOXA were obtained through enzymatic crosslinking of PEOXA-peptide conjugates.

A 5% (w/v) alginate stock solution was prepared by dissolving sodium alginate (Alg) (PRONOVA UP-MVG) in 150 mM HEPES buffer at 90°C. This temperature enabled a faster dissolution of alginate and ensured sterilization of the solution. The single network Alg hydrogels were prepared by casting a 1% (w/v) Alg solution within PDMS rings (6 mm of external and 4 mm of internal diameter), then the casted Alg solutions were covered with filter paper, and finally crosslinked by adding 100 mM CaCl₂ solutions.

Double network hydrogels (DN-PEOXA-Alg) were obtained by combining pre-hydrogel mixtures of PEOXA with those containing Alg and subsequently adding a solution of 10 µM SA, and later on 100 mM CaCl₂.

DN-PEOXA-Alg were additionally complemented with cellulose nanofibrils (CNF) (yielding DN-PEOXA-Alg-CNF), by following a similar preparation protocol while adding different concentrations of CNF to the pre-hydrogel mixtures, that is 0.5, 1.0, 1.5 and 2.0 % (w/v).

Rheological Measurements

Gelation kinetics were measured using an Anton Paar MCR 301 Rheometer with a 20 mm plate-plate geometry and a base floor maintained at 25°C. Time sweep was performed to measure the storage modulus with 2 % strain at 1 Hz frequency during 20 s steps for 60 min, with a gap between plates maintained at 0.2 mm. The storage and loss moduli of single and double networks were obtained from these measurements. Shear thinning and shear recovery measurements were additionally performed on the different pre-hydrogel mixtures. Shear thinning experiments were performed to calculate the viscosity of the hydrogels at a frequency 1 rad s⁻¹ with logarithmic increase in shear rate, and keeping a gap between plates of 0.2 mm. In order to measure the shear recovery, pre-hydrogel mixtures were exposed to 0.5% strain for 200 s, 1000% strain for 10s, 0.5%

strain for 600 s, 1000% strain for 10s, and 0.5% strain for 600 s, while maintaining a gap of 0.6 mm between the rheometer plates.

Mechanical Testing

Compression tests were performed using a texture analyzer (TA.XT plus, Texture Analyzer, Stable Micro Systems), where 15 μl of pre-hydrogel solutions were casted within PDMS rings (6 mm of external and 4 mm of internal diameter) and then crosslinked by adding a solution containing 100 mM CaCl_2 and 10 μM SA. Unconfined compression was applied to the specimens using a 500 g load cell, reaching a final strain of up to 15% at the rate of 0.01 mm s^{-1} . The Young's moduli (E) were calculated from the slope of the linear region of the stress-strain curves.

Cell Studies

Human auricular chondrocytes (hACs) were isolated from biopsies with approval of the local ethics committee (BASEC Nr. 2017-02101) and patient consent. Cartilage pieces were first washed with PBS containing 50 $\mu\text{g mL}^{-1}$ gentamycin and cut into smaller pieces (1–2 mm^3). The minced cartilage was then enzymatically digested with collagenase (0.12% w/v, C6885) in DMEM expansion media for 5–6 h at 37 $^\circ\text{C}$. The obtained chondrocyte suspension was then filtered with 100 μm cell strainers to remove undissolved cartilage pieces. The cells were pelleted, re-suspended in recovery medium at 2.5×10^6 cells mL^{-1} and frozen at passage 1 until further use. For cell viability experiments, the cells were cultured in FalconTM 5 layered flasks for about 2 weeks before they were trypsinised and encapsulated in the hydrogels. The viability of the cells before encapsulation was measured using trypan blue exclusion. For cell encapsulation experiments 300 μl of pre-hydrogel mixtures loaded with 10^7 cells mL^{-1} were homogeneously mixed before crosslinking. The crosslinking was initiated by quickly adding SA into the hACs-containing pre-

hydrogel mixture. After crosslinking was initiated, 15 μl of the mixture was quickly casted into cylindrical PDMS rings. Then the mixtures were incubated for 1 hour at 37 °C, adding 100 mM CaCl_2 solution to complete the crosslinking process, and they were finally incubated in chondrogenic medium (DMEM supplemented with 10 ng mL^{-1} transforming growth factor $\beta 3$ (TGF- $\beta 3$, Peprotech), 100 nM dexamethasone, 50 $\mu\text{g mL}^{-1}$ L-ascorbate-2-phosphate, 40 $\mu\text{g mL}^{-1}$ proline, 1% penicillin–streptomycin, and 1% ITS+ Premix).

hACs-loaded hydrogels and bioprinted grids were imaged for cell viability using Leica SP8 Multiphoton Microscopy with (25x water immersion objective). The samples were stained using calcein AM 2 μM and propidium iodide (PI) 6.6 $\mu\text{g mL}^{-1}$ dissolved in DMEM, incubated for 1 hour at 37 °C with 5% CO_2 and washed with fresh DMEM medium. The images shown in this study were at 50 μm from the sample's surface and were imaged for a total z-stack size of 100 μm for all the samples. To image the whole bioprinted grid structure, tiles were stitched together using Zen software on an Axio Observer with Apatome, Carl Zeiss, Oberkochen, Germany). Finally, the raw images were processed using ImageJ and Maximum Intensity Projection (MIP) stacks were combined and live/dead cells were counted for cell viability.

3D Printing and bioprinting

DN hydrogel grids were designed using Autodesk Fusion 360, and G-codes were generated using Slicer software for designing 3D structures. 3D printing of grids was performed using an extrusion-based printer (Cellink, INKREDIBLE. Gothenburg, Sweden). The printing pressure was in the range 18-21 kPa and the diameter of the needle was 410 μm .

10^7 cells mL^{-1} were added to the pre-hydrogels for bioprinting. Initially, hACs were cultured for 14 days, trypsinised and centrifuged at 500 ref for 5 min. The pre-hydrogel mixture was directly

pipetted into sterile 5 mL Eppendorf tubes containing hACs, and mixed until the cells were evenly distributed. This mixture was then loaded into a 3 mL sterile syringe (BD Life Sciences) and mounted on the INKREDIBLE printer, while maintaining the same printing conditions as indicated above, with the exception of the printing pressure, which was set to 28 kPa in the presence of hACs. The printed grids were then crosslinked by immersing them in a solution containing 100mM CaCl₂ and 10 μM SA for one hour, after which the constructs were finally incubated in cell culture medium (DMEM with 10% v/v FBS, 2 mM L-glutamine, and 10 μg mL⁻¹ gentamycin).

Statistical Analysis

Three samples for each hydrogel type were analyzed, including cell viability analysis, whereby 3 measurements were done on each sample (n=3). The statistics and plotting were done using OriginPro 8 software. Multiple samples were checked for significance using one-way ANOVA and Tukey's multiple comparison post-hoc test.

RESULTS AND DISCUSSION

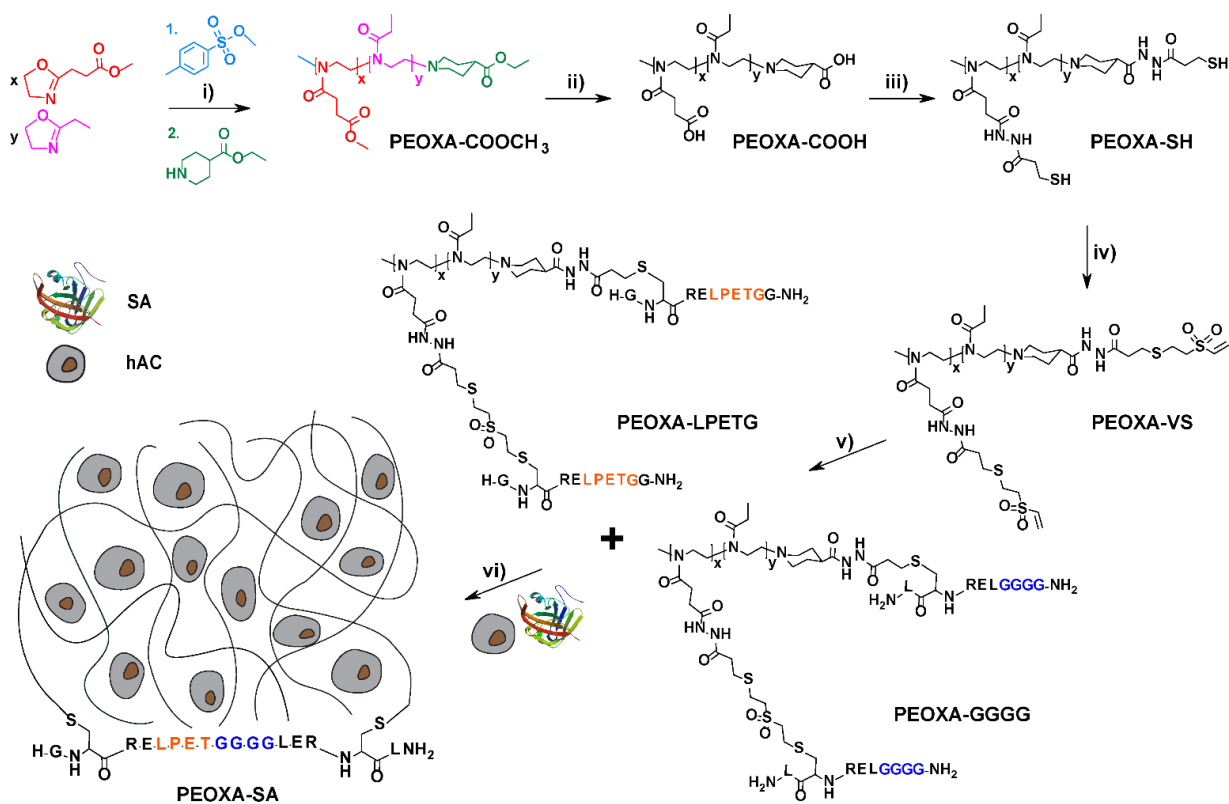
Synthesis and Characterization of PEOXA-peptide Conjugates

PEOXA-peptide conjugates that were used as substrates for the subsequent SA-assisted enzymatic crosslinking were synthesized by CROP of 85 mol% of 2-ethyl-2-oxazoline (EOXA) and 15 mol% of 2-methoxycarboxyethyl-2-oxazoline (MestOXA), followed by post-functionalization. *p*-toluenesulfonate (MeOTs) was used as electrophilic initiator, and an excess of ethyl isonipecotate was employed for terminating the polymerization (Scheme 1i), yielding copolymers with a random distribution of methyl ester side chains and an ethyl ester on one chain end, abbreviated as PEOXA-COOCH₃ (Scheme 1i). The composition of PEOXA-COOCH₃ was confirmed by ¹H-

NMR spectroscopy (Figure S5), while size exclusion chromatography (SEC) indicated a number average molecular weight (M_n) of 16.9 kDa and a polydispersity index (PDI) of 1.14, suggesting a controlled co-polymerization process (Figure S9 and Table S1). The methyl ester side chains, as well as the ethyl ester chain ends were hydrolyzed under alkaline conditions, yielding free carboxylic acids-bearing PEOXA (PEOXA-COOH) (Scheme 1ii). 3,3'-dithiobis(propanoic dihydrazide) (DTPHY) was coupled to the COOH moieties, through EDC/hydrazide-mediated coupling, followed by reduction of the disulfide moieties within DTPHY, yielding thiolated PEOXA (PEOXA-SH) (Scheme 1iii). Thiol-Michael addition was subsequently employed to functionalize PEOXA-SH with vinyl sulfonate, yielding PEOXA-VS (Scheme 1iv, Figure S6). Finally, thiol-bearing oligopeptide fragments reactive towards SA were coupled to PEOXA-VS by thiol-Michael addition. In particular, two different PEOXA conjugates were obtained, one featuring SA donor peptides GCRE-LPETGG-NH₂ (NH₂ refers to amidated C-terminus), which includes the recognition sequence LPETG, and were indicated as PEOXA-LPETG, and one containing SA acceptor peptides GGGG-LERCL-NH₂, including the nucleophilic oligoglycine GGGG, and which were indicated as PEOXA-GGGG and (Scheme 1v and Figure S7 and S8). The quantitative functionalization of PEOXA-VS with the different oligopeptides was confirmed by ¹H-NMR, which highlighted the complete disappearance of the proton peaks corresponding to the VS functions upon conjugation with the peptide fragments, as reported in Figure S7 and S8. Mixtures of PEOXA-LPETG and PEOXA-GGGG were subsequently reacted in the presence of SA, yielding a covalently crosslinked network, as reported in Scheme 1vi.

Scheme 1. Synthesis of PEOXA-peptide conjugates and their SA-catalysed crosslinking reaction. (i) Copolymerization of EOXA (in pink) with 15 mol% of MestOXA (in red) by CROP was performed in dry ACN at 80°C for 48 h. The polymerization was initiated by MeOTs, and termination was carried out in the presence of an excess of ethyl isonipecotate at room temperature

for 24 h, resulting in PEOXA-COOCH₃. **(ii)** The hydrolysis of ester side chains and chain ends was performed in 1 M NaOH for 24 h at room temperature, yielding PEOXA-COOH. **(iii)** PEOXA-SH was obtained by reacting PEOXA-COOH with EDC-HCl and DTPHY at pH 4.5 for 4 h, followed by reduction of disulfide groups by TCEP-HCl for 16 h at room temperature. **(iv)** PEOXA-VS was synthesized by reacting PEOXA-SH with DVS in aqueous TEOA buffer at pH 8 for 30 min. **(v)** The PEOXA-peptide conjugates, namely PEOXA-LPETG and PEOXA-GGGG were finally synthesized from PEOXA-VS via Michael-thiol addition, specifically by reacting the cysteine's thiol group of GCRELPE_xTGG-NH₂ and GGGGLERCL-NH₂, respectively with vinyl sulfones of the PEOXA-VS. **(vi)** SA-mediated ligation of the two SA-recognition peptides (LPETG and GGGG) coupled to PEOXA resulting in crosslinking of the PEOXA chains and eventually hydrogel formation in the presence of hACs under physiological conditions.



Synthesis and Characterization of DN Hydrogels

The formation of all the different hydrogels, including enzymatically crosslinked PEOXA, alginate (Alg), PEOXA-Alg DN hydrogels, and DN hydrogel supplemented with CNF (DN-CNF), was monitored by rheology (Figure 1a). SA-mediated crosslinking of 1:1 solutions of PEOXA-LPETG

and PEOXA-GGGG PEOXA with a total polymer concentration of 5 % (w/v), and employing 10 μM SA resulted in the formation of a soft hydrogel reaching an equilibrium storage modulus (G') of around 300 Pa in 30 min. The low recorded G' was probably due to the reversibility of the SA-catalyzed transpeptidation reaction, leading to incomplete crosslinking of the network.^{52,53} Ionic crosslinking of a 1 % (w/v) solution of Alg through Ca^{2+} led to an hydrogel matrix with an order of magnitude higher G' , which at equilibrium reached 3 kPa (Figure 1b). The combination of PEOXA and Alg hydrogels yielded a DN with improved mechanical properties and viscoelasticity.⁵⁴ DN PEOXA-Alg hydrogels showed a G' at equilibrium of 8 kPa, which is more than twofold higher than the combined values of G' for the single networks (Figure 1b), and indicated that chain entanglement between the two polymer types within the DN^{19,55} significantly strengthened the mechanical properties of the obtained matrix. It is also important to emphasize that SA-mediated crosslinking of PEOXA-peptide conjugates did not seem affected by the presence of the Alg-based physical network, as it was suggested by the similar gelation kinetics observed for the DN compared that recorded in pure PEOXA hydrogels.

Similar results were obtained when the mechanical properties of PEOXA, Alg and DN PEOXA-Alg hydrogels were compared by unconfined compression testing (Figure 1c and 1d). The DN hydrogel reached a compressive modulus of ~ 30 kPa, which was three and ten times higher than those recorded for the Alg and PEOXA hydrogels, respectively (Figure 1d).

Finally, the addition of CNF to the DN PEOXA-Alg hydrogel (DN PEOXA-Alg-CNF), which improved the printability of the matrix (*vide infra*), resulted in an additional increment of G' , which reached 14 kPa at equilibrium. However, after the addition of CNF, no further increase in the compressive modulus was observed.

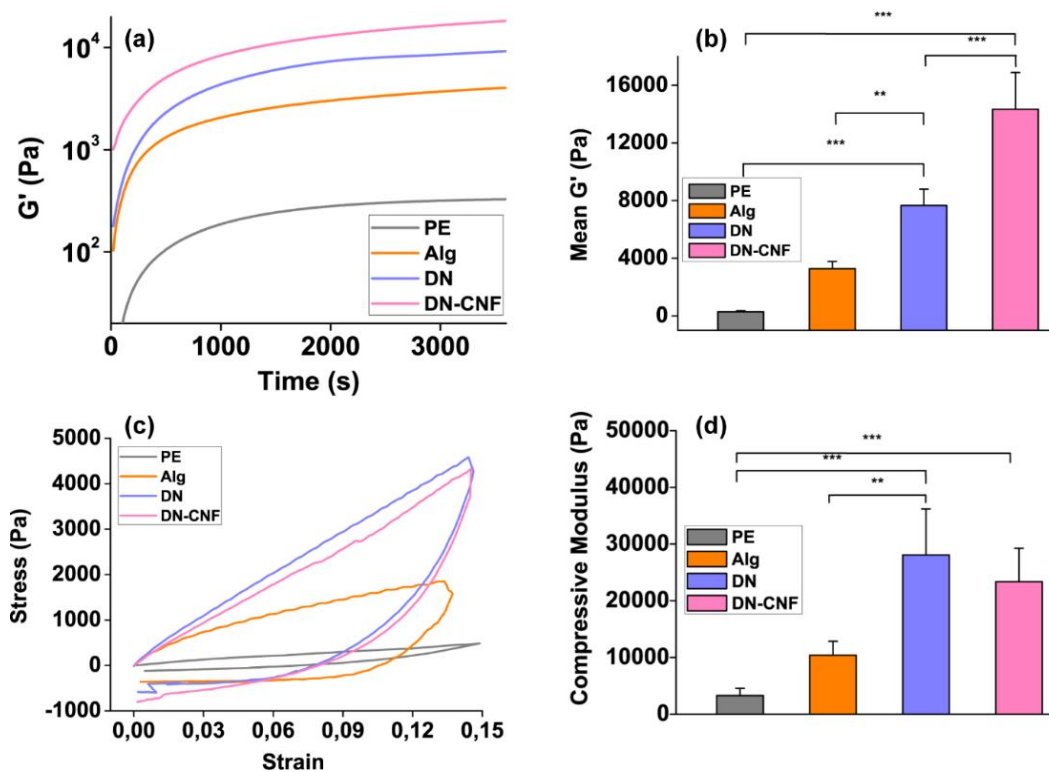


Figure 1. Gelation kinetics and compressive stiffness for PEOXA, Alg, DN PEOXA-Alg and DN PEOXA-Alg-CNF hydrogels. (a) Representative gelling curves for the different hydrogels showing the build-up of G' over time. (b) Mean G' at equilibrium (recorded after 60 min) for the different hydrogels. (c) Stress-strain curves of the different hydrogels. (d) Compressive modulus recorded as the slope of the linear region of the stress-strain curve.

3D Printing of DN Hydrogels

A precursor hydrogel bioink requires shear thinning and shear recoverable properties in order to be efficiently extruded, and to retain its structured shape after the 3D printing process.⁵⁶⁻⁵⁸ Hence, the rheological properties of the different polymer mixtures used as precursor formulations for the hydrogels investigated prior to the 3D bioprinting experiments. As reported in Figure 2a, pure PEOXA solutions (5% w/v) showed very low viscosity at room temperature. Pure Alg solutions (1 % w/v) showed an increment in viscosity, although the recorded zero-shear viscosity was still rather low, and these pre-hydrogel mixtures did not display shear thinning behaviour (that is, a decrease in viscosity with increasingly applied shear rate).

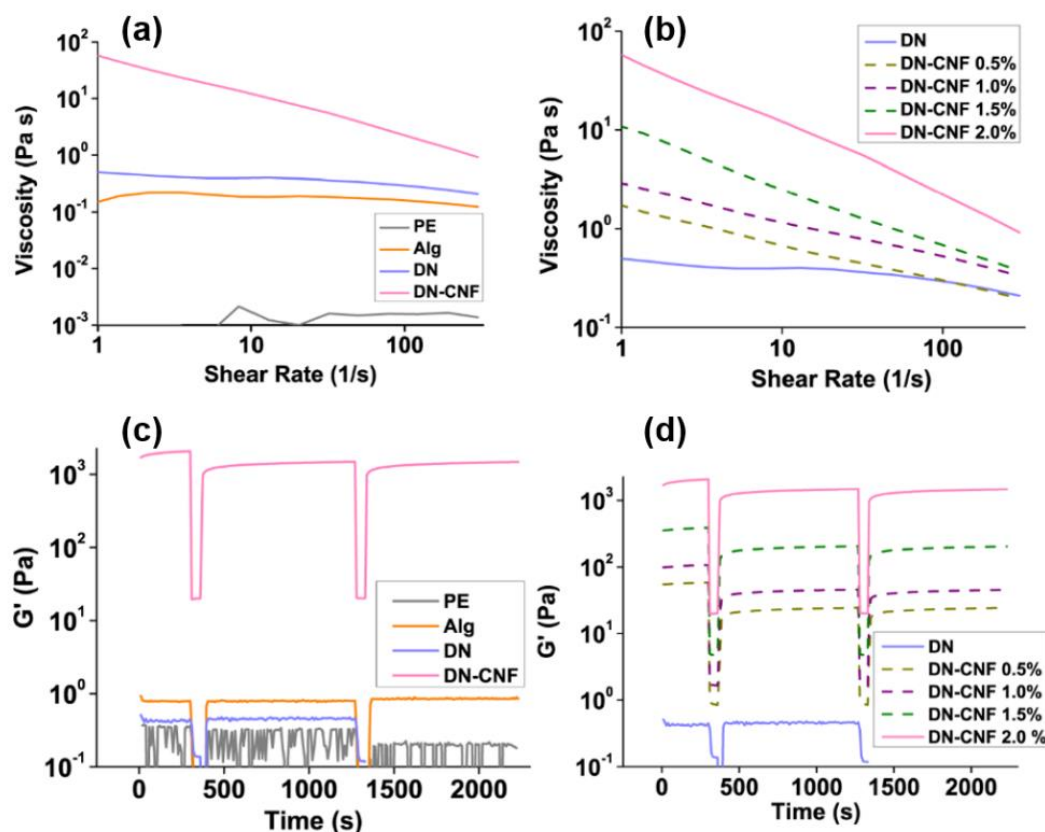


Figure 2. Rheological properties of the different polymer mixtures used as bioprinting materials. (a) Flow curves showing the change in viscosity with applied shear rate. (b) Flow curves of DN hydrogel alone and supplemented with different concentrations of CNF. (c) Shear recovery of inks (c), shear recovery of various concentrations of CNF within DN (d).

Addition of 5% PEOXA (w/v) to 1% Alg solution (w/v) gave a slight increment in zero-shear viscosity, probably due to the increase in the total polymer concentration within the pre-hydrogel solution. However, the mixture used for the formation of DN hydrogel did not display shear thinning (Figure 2a, blue curve), and thus was not ideal for successful bioprinting. In order to enhance the printability of DN hydrogels, different amounts of CNF were added to PEOXA-Alg mixtures (Figure 2a and 2b). An increment in the CNF content from 0.5 to 2.0 % (w/v) was mirrored by a concomitant increase in the zero-shear viscosity from 35 to 2600 Pa s, and resulted in a shear thinning solution, when compared to the DN pre-hydrogel mixture alone (Figure 2b).

Moreover, the addition of CNF to PEOXA-Alg solutions resulted in mixtures characterized by a fast shear recovery behaviour, reaching more than 80 % of the initial storage modulus after two high-strain phases (Figure 2c). The observed shear recovery could be additionally adjusted by varying the CNF content within DN ink, as shown in Figure 2d.

PEOXA-Alg-CNF mixtures could be efficiently 3D printed to yield a grid of pre-hydrogel solution displaying good shape fidelity, also prior to crosslinking (Figure 3a). Subsequent incubation in a buffer containing CaCl_2 and SA for one hour resulted in the formation of 3D printed DN hydrogel (Figure 3b). It is important to emphasize that the spaces within the printed construct remained intact without rupture or closure, probably as a direct consequence of the shear recovery character of PEOXA-Alg-CNF pre-hydrogel solutions. In addition, the 3D printed DN hydrogels showed a good structural stability and resistance to tensile stress, as demonstrated in Figure 3c where a manual stretching test was reported.

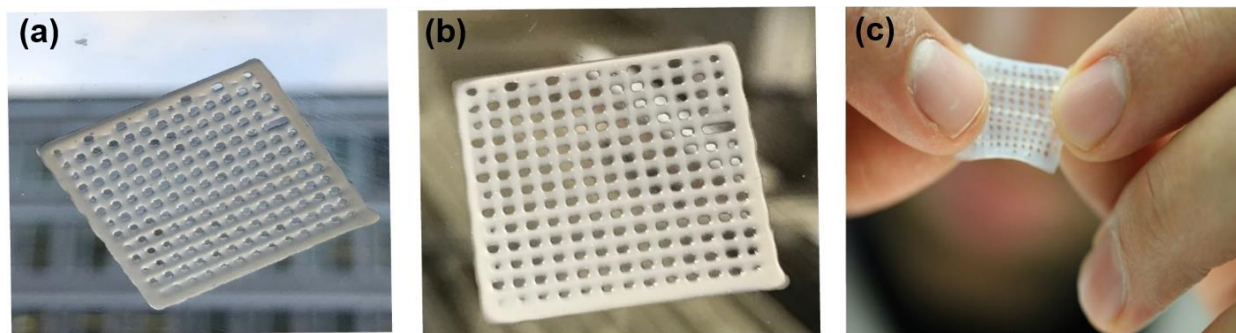


Figure 3: 3D printing with the DN-CNF ink. (a) 3D printed grids ($20 \times 20 \times 0.4 \text{ mm}^3$) after the extrusion process, before crosslinking. (b) The same printed grid after one-hour incubation with crosslinking solution. (c) Stretching of the printed DN-CNF hydrogel.

Biocompatibility and 3D Bioprinting

The cytocompatibility of PEOXA and Alg hydrogels, and that of DN PEOXA-Alg and PEOXA-Alg-CNF hydrogels was subsequently tested in the presence of hACs, which were encapsulated

within the polymer networks during SA-mediated enzymatic and ionic crosslinking. Generally, high cell viability of $\sim 90\%$ at 1, 7, and 21 days post-encapsulation was measured for all the hydrogels, with the exception of PEOXA, which showed a significantly lower cell viability of $74 \pm 3\%$ after 24 hours after encapsulation, although this increased to $89 \pm 2\%$ following one week of culture (Figure 4a and 4b). PEOXA-Alg DN hydrogels also showed a cell viability higher than 90%, even after 21 days of encapsulation, while the incorporation of CNF into the DN formulation did not adversely affect hACs.^{59,60}

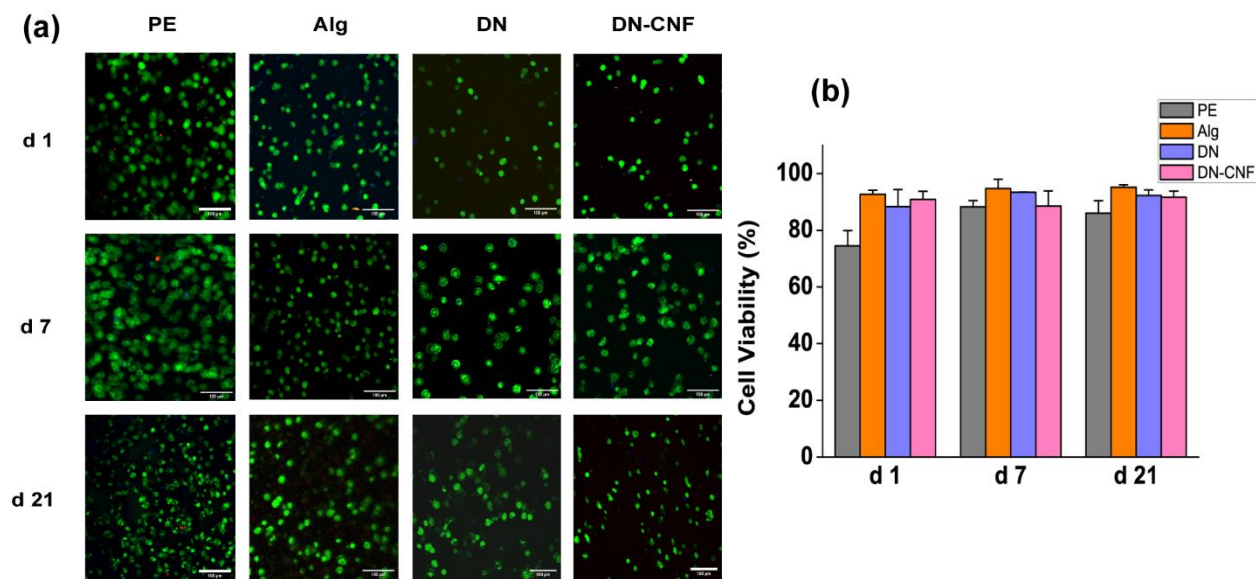
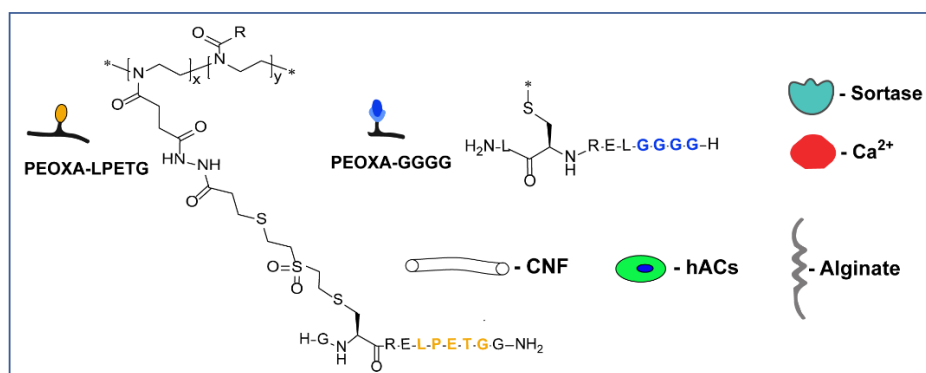
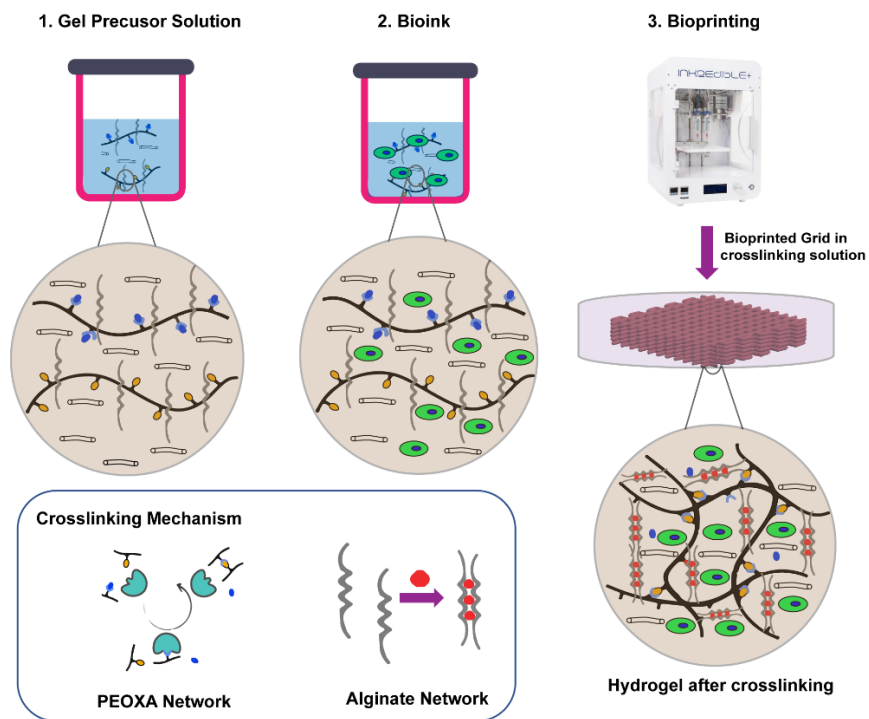


Figure 4. Cytocompatibility of encapsulated hACs in hydrogels. (a) Two-photon microscopy imaging of live cells in green (calcein AM stains cytoplasm of viable cells) and dead cells in red (propidium iodide stains nuclei of dead cells) 1, 7 and 21 days post-encapsulation, as maximum intensity projections over $100\ \mu\text{m}$. Scale bars: $100\ \mu\text{m}$. (b) Quantifications of the hAC viability at 1, 7, and 21 days (d1, d7 and d21) post-encapsulation for the different gels. SD $n=3$.

The pre-hydrogel mixture including PEOXA, Alg and CNF was subsequently printed in the presence of hACs, following the procedures summarized in Scheme 2.

The presence of hACs within the printable formulation only slightly affected the 3D printing parameters, with the printing pressure being increased from 20 to 28 kPa, in order to compensate for the higher viscosity of the bioink with respect to the cell-free pre-hydrogel mixture.

Printing the DN hydrogels in the presence of hACs did not affect the structural stability of the obtained grid constructs, and maintained the shape fidelity of the process (Figure 5a and 5b), suggesting a good shear recovery behaviour even in the presence of cells. Although 3D bioprinting processes were previously reported to have detrimental effects on cells' survival, mainly due to the shear forces exerted on cells during extrusion,⁶¹ bioprinting of hACs with PEOXA-Alg-CNF resulted in excellent cell viability ($90 \pm 2\%$) both after 1 and 7 days (Figure 5c and 5d).



Scheme 2. 3D bioprinting process using PEOXA-Alg-CNF mixture and hACs. (1) The hydrogel precursor solution contains PEOXA-LPETG and PEOXA-GGGG, both at 2.5 % (w/v), and thus included a total POEXA concentration of 5%. Alg concentration was set to 1 % (w/v) and CNF content was 2 % (w/v) in Tris buffer. (2) The bioink used for printing featured PEOXA-Alg-CNF complemented with hACs. (3) The fabrication of 3D-printed hydrogel grids was carried out by first extruding the pre-hydrogel mixture with hACs, and subsequently crosslinking the printed bioink via incubation with SA and Ca^{2+} solutions.

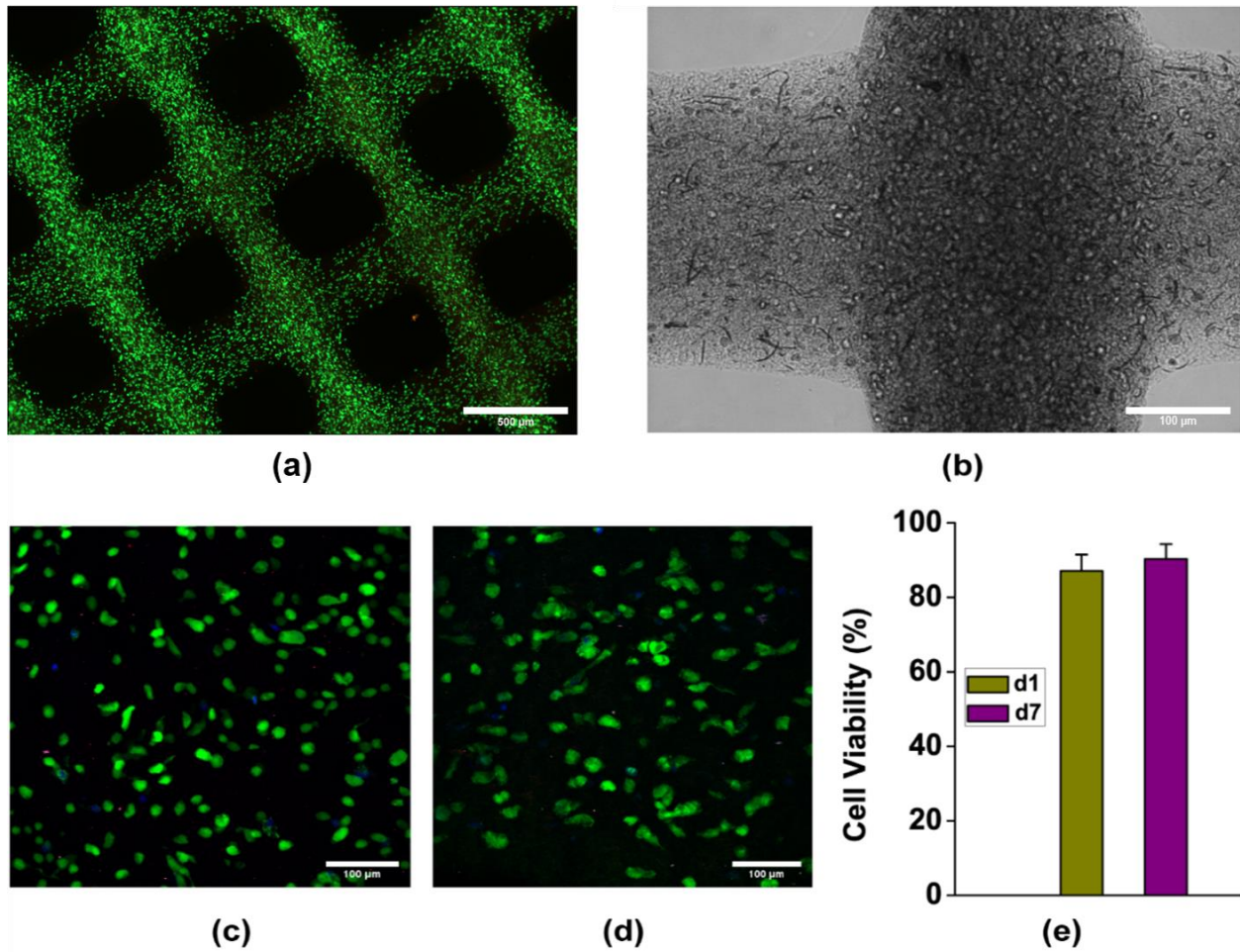


Figure 5. (a) Wide-field fluorescence micrographs depicting hACs stained with calcein/propidium iodide encapsulated within PEOXA-Alg-CNF DN hydrogels after 3D bioprinting. (b) Optical micrographs of 3D bioprinted grids highlight the presence of CNF. (c) Two-photon microscopy images highlighting hACs within 3D printed constructs after 1 day and (d) after 7 days post-printing. (e) Quantification of hAC viability within 3D bioprinted grids after 1 and 7 days (d1 and d7) post-printing; SD n=3 for all conditions.

Conclusions

The fabrication of DN hydrogels including enzymatically crosslinked PEOXAs and Alg-based physical networks generated matrices with improved mechanical properties with respect to the corresponding single-network PEOXA- and Alg-based hydrogels. Incorporation of hACs within DN hydrogels resulted in excellent cell viability after three weeks since encapsulation, highlighting these materials as suitable supports for 3D cell culture and tissue engineering.

When CNF are added to PEOXA-Alg pre-hydrogel mixtures, the viscosity of the solutions significantly increased, while the shear thinning and recovery properties were substantially enhanced, making these formulations applicable for extrusion-based 3D printing. PEOXA-Alg-CNF mixtures could thus be printed to yield 3D structures featuring good shape fidelity, which were later on quickly crosslinked by incubation in SA/Ca²⁺ solutions, generating 3D DN hydrogels. Pre-hydrogel formulations were finally complemented with hACs, and subsequently bioprinted to yield 3D DN grids incorporating cells, which showed a viability higher than 90% over one week after printing.

The proposed formulations extend the applicability of PAOXAs in designing tissue engineered scaffolds, and additionally demonstrate that SA-mediated enzymatic crosslinking is a versatile and extremely fast method not only to generate DN hydrogels, but also to rapidly crosslink 3D printed structures. Relevantly, this crosslinking method also ensures significantly high viability for cells encapsulated within PAOXA-based networks, if compared to other non-bio-orthogonal crosslinking methods, thus enabling the generation of PAOXA hydrogels showing the highest biocompatibility among compositionally similar materials.^{32,62–64}

References

- (1) Lutolf, M. P.; Hubbell, J. A. Synthetic Biomaterials as Instructive Extracellular Microenvironments for Morphogenesis in Tissue Engineering. *Nat. Biotechnol.* **2005**, *23* (1), 47–55.
- (2) Place, E. S.; George, J. H.; Williams, C. K.; Stevens, M. M. Synthetic Polymer Scaffolds for Tissue Engineering. *Chem. Soc. Rev.* **2009**, *38* (4), 1139–1151.
- (3) Tibbitt, M. W.; Anseth, K. S. Hydrogels as Extracellular Matrix Mimics for 3D Cell Culture.

- Biotechnol. Bioeng.* **2009**, *103* (4), 655–663.
- (4) Drury, J. L.; Mooney, D. J. Hydrogels for Tissue Engineering: Scaffold Design Variables and Applications. *Biomaterials* **2003**, *24* (24), 4337–4351.
 - (5) Lin, C. C.; Anseth, K. S. PEG Hydrogels for the Controlled Release of Biomolecules in Regenerative Medicine. *Pharm. Res.* **2009**, *26* (3), 631–643.
 - (6) Chaudhuri, O.; Gu, L.; Klumpers, D.; Darnell, M.; Bencherif, S. A.; Weaver, J. C.; Huebsch, N.; Lee, H.; Lippens, E.; Duda, G. N.; et al. Hydrogels with Tunable Stress Relaxation Regulate Stem Cell Fate and Activity. *Nat. Mater.* **2015**, *15*, 326.
 - (7) McKinnon, D. D.; Domaille, D. W.; Cha, J. N.; Anseth, K. S. Biophysically Defined and Cytocompatible Covalently Adaptable Networks as Viscoelastic 3D Cell Culture Systems. *Adv. Mater.* **2014**, *26* (6), 865–872.
 - (8) Cameron, A. R.; Frith, J. E.; Cooper-White, J. J. The Influence of Substrate Creep on Mesenchymal Stem Cell Behaviour and Phenotype. *Biomaterials* **2011**, *32* (26), 5979–5993.
 - (9) Chaudhuri, O.; Gu, L.; Darnell, M.; Klumpers, D.; Bencherif, S. A.; Weaver, J. C.; Huebsch, N.; Mooney, D. J. Substrate Stress Relaxation Regulates Cell Spreading. *Nat. Commun.* **2015**, *6*, 6365.
 - (10) Tang_et_al-2018-Advanced_Science_Adaptable Fast Relaxing Boronate-Based Hydrogels for Probing Cell–Matrix Interactions.Pdf.
 - (11) Khetan, S.; Guvendiren, M.; Legant, W. R.; Cohen, D. M.; Chen, C. S.; Burdick, J. A. Degradation-Mediated Cellular Traction Directs Stem Cell Fate in Covalently Crosslinked

- Three-Dimensional Hydrogels. *Nat. Mater.* **2013**, *12*, 458.
- (12) Sahoo, S.; Chung, C.; Khetan, S.; Burdick, J. A. Hydrolytically Degradable Hyaluronic Acid Hydrogels with Controlled Temporal Structures. *Biomacromolecules* **2008**, *9* (4), 1088–1092.
- (13) Lou, J.; Stowers, R.; Nam, S.; Xia, Y.; Chaudhuri, O. Stress Relaxing Hyaluronic Acid-Collagen Hydrogels Promote Cell Spreading, Fiber Remodeling, and Focal Adhesion Formation in 3D Cell Culture. *Biomaterials* **2018**, *154*, 213–222.
- (14) Rosales, A. M.; Vega, S. L.; DelRio, F. W.; Burdick, J. A.; Anseth, K. S. Hydrogels with Reversible Mechanics to Probe Dynamic Cell Microenvironments. *Angew. Chemie Int. Ed.* **2017**, *56* (40), 12132–12136.
- (15) Shih, H.; Lin, C.-C. Tuning Stiffness of Cell-Laden Hydrogel via Host–Guest Interactions. *J. Mater. Chem. B* **2016**, *4* (29), 4969–4974.
- (16) Gong, J. P.; Katsuyama, Y.; Kurokawa, T.; Osada, Y. Double-Network Hydrogels with Extremely High Mechanical Strength. *Adv. Mater.* **2003**, *15* (14), 1155–1158.
- (17) Haque, M. A.; Kurokawa, T.; Gong, J. P. Super Tough Double Network Hydrogels and Their Application as Biomaterials. *Polymer (Guildf)*. **2012**, *53* (9), 1805–1822.
- (18) Yasuda, K.; Gong, J. P.; Katsuyama, Y.; Nakayama, A.; Tanabe, Y.; Kondo, E.; Ueno, M.; Osada, Y. Biomechanical Properties of High-Toughness Double Network Hydrogels. *Biomaterials* **2005**, *26* (21), 4468–4475.
- (19) Tsukeshiba, H.; Huang, M.; Na, Y. H.; Kurokawa, T.; Kuwabara, R.; Tanaka, Y.; Furukawa, H.; Osada, Y.; Gong, J. P. Effect of Polymer Entanglement on the Toughening of Double

- Network Hydrogels. *J. Phys. Chem. B* **2005**, *109* (34), 16304–16309.
- (20) Webber, R. E.; Creton, C.; Brown, H. R.; Gong, J. P. Large Strain Hysteresis and Mullins Effect of Tough Double-Network Hydrogels. *Macromolecules* **2007**, *40* (8), 2919–2927.
- (21) Hoogenboom, R. Poly(2-Oxazoline)s: A Polymer Class with Numerous Potential Applications. *Angew. Chemie - Int. Ed.* **2009**, *48* (43), 7978–7994.
- (22) Adams, N.; Schubert, U. S. Poly(2-Oxazolines) in Biological and Biomedical Application Contexts. *Adv. Drug Deliv. Rev.* **2007**, *59* (15), 1504–1520.
- (23) Boerman, M. A.; Roozen, E.; Sánchez-Fernández, M. J.; Keereweer, A. R.; Félix Lanao, R. P.; Bender, J. C. M. E.; Hoogenboom, R.; Leeuwenburgh, S. C.; Jansen, J. A.; Van Goor, H.; et al. Next Generation Hemostatic Materials Based on NHS-Ester Functionalized Poly(2-Oxazoline)s. *Biomacromolecules* **2017**, *18* (8), 2529–2538.
- (24) Weydert, S.; Zürcher, S.; Tanner, S.; Zhang, N.; Ritter, R.; Peter, T.; Aebbersold, M. J.; Thompson-Steckel, G.; Forró, C.; Rottmar, M.; et al. Easy to Apply Polyoxazoline-Based Coating for Precise and Long-Term Control of Neural Patterns. *Langmuir* **2017**, *33* (35), 8594–8605.
- (25) Wilson, P.; Ke, P. C.; Davis, T. P.; Kempe, K. Poly(2-Oxazoline)-Based Micro- and Nanoparticles: A Review. *Eur. Polym. J.* **2017**, *88*, 486–515.
- (26) Viegas, T. X.; Bentley, M. D.; Harris, J. M.; Fang, Z.; Yoon, K.; Dizman, B.; Weimer, R.; Mero, A.; Pasut, G.; Veronese, F. M. Polyoxazoline: Chemistry, Properties, and Applications in Drug Delivery. *Bioconjug. Chem.* **2011**, *22* (5), 976–986.
- (27) Luxenhofer, R.; Han, Y.; Schulz, A.; Tong, J.; He, Z.; Kabanov, A. V.; Jordan, R. Poly (2-

- Oxazoline)s as Polymer Therapeutics. *Macromol. Rapid Commun.* **202AD**, 33, 1613–1631.
- (28) Matsumoto, T.; Isogawa, Y.; Tanaka, T.; Kondo, A. Streptavidin-Hydrogel Prepared by Sortase A-Assisted Click Chemistry for Enzyme Immobilization on an Electrode. *Biosens. Bioelectron.* **2018**, 99 (July 2017), 56–61.
- (29) Lorson, T.; Lübtow, M. M.; Wegener, E.; Haider, M. S.; Borova, S.; Nahm, D.; Jordan, R.; Sokolski-Papkov, M.; Kabanov, A. V.; Luxenhofer, R. Poly(2-Oxazoline)s Based Biomaterials: A Comprehensive and Critical Update. *Biomaterials* **2018**, 178, 204–280.
- (30) Benetti, E. M.; Divandari, M.; Ramakrishna, S. N.; Morgese, G.; Yan, W.; Trachsel, L. Loops and Cycles at Surfaces: The Unique Properties of Topological Polymer Brushes. *Chem. - A Eur. J.* **2017**, 23 (51), 12433–12442.
- (31) Morgese, G.; Shirmardi Shaghasemi, B.; Causin, V.; Zenobi-Wong, M.; Ramakrishna, S. N.; Reimhult, E.; Benetti, E. M. Next-Generation Polymer Shells for Inorganic Nanoparticles Are Highly Compact, Ultra-Dense, and Long-Lasting Cyclic Brushes. *Angew. Chemie - Int. Ed.* **2017**, 56 (16), 4507–4511.
- (32) Farrugia, B. L.; Kempe, K.; Schubert, U. S.; Hoogenboom, R.; Dargaville, T. R. Poly (2-Oxazoline) Hydrogels for Controlled Fibroblast Attachment. *Biomacromolecules* **2013**, 14, 2724–2732.
- (33) Dargaville, T. R.; Hollier, B. G.; Shokohmand, A.; Hoogenboom, R. Poly(2-Oxazoline) Hydrogels as next Generation Three-Dimensional Cell Supports. *Cell Adhes. Migr.* **2014**, 8 (2), 88–93.
- (34) Ton-That, H.; Liu, G.; Mazmanian, S. K.; Faull, K. F.; Schneewind, O. Purification and

- Characterization of Sortase, the Transpeptidase That Cleaves Surface Proteins of Staphylococcus Aureus at the LPXTG Motif. *Proc. Natl. Acad. Sci.* **1999**, *96* (22), 12424–12429.
- (35) Ilangovan, U.; Ton-That, H.; Iwahara, J.; Schneewind, O.; Clubb, R. T. Structure of Sortase, the Transpeptidase That Anchors Proteins to the Cell Wall of Staphylococcus Aureus. *Proc. Natl. Acad. Sci.* **2001**, *98* (11), 6056–6061.
- (36) Moreira Teixeira, L. S.; Feijen, J.; van Blitterswijk, C. A.; Dijkstra, P. J.; Karperien, M. Enzyme-Catalyzed Crosslinkable Hydrogels: Emerging Strategies for Tissue Engineering. *Biomaterials* **2012**, *33* (5), 1281–1290.
- (37) Anjum, F.; Lienemann, P. S.; Metzger, S.; Biernaskie, J.; Kallos, M. S.; Ehrbar, M. Enzyme Responsive GAG-Based Natural-Synthetic Hybrid Hydrogel for Tunable Growth Factor Delivery and Stem Cell Differentiation. *Biomaterials* **2016**, *87*, 104–117.
- (38) Hu, J.; Zhang, G.; Liu, S. Enzyme-Responsive Polymeric Assemblies, Nanoparticles and Hydrogels. *Chem. Soc. Rev.* **2012**, *41* (18), 5933.
- (39) Broguiere, N.; Isenmann, L.; Zenobi-Wong, M. Novel Enzymatically Cross-Linked Hyaluronan Hydrogels Support the Formation of 3D Neuronal Networks. *Biomaterials* **2016**, *99*, 47–55.
- (40) Broguiere, N.; Cavalli, E.; Salzmann, G. M.; Applegate, L. A.; Zenobi-Wong, M. Factor XIII Cross-Linked Hyaluronan Hydrogels for Cartilage Tissue Engineering. *ACS Biomater. Sci. Eng.* **2016**, *2* (12), 2176–2184.
- (41) Broguiere, N.; Formica, F.; Barreto, G.; Zenobi-Wong, M. Sortase A as a Cross-Linking

Enzyme in Tissue Engineering. *Acta Biomater.* **2018**.

- (42) Guimaraes, C. P.; Witte, M. D.; Theile, C. S.; Bozkurt, G.; Kundrat, L.; Blom, A. E. M.; Ploegh, H. L. Site-Specific C-Terminal and Internal Loop Labeling of Proteins Using Sortase-Mediated Reactions. *Nat. Protoc.* **2013**, *8* (9), 1787–1799.
- (43) Phelps, E. A.; Enemchukwu, N. O.; Fiore, V. F.; Sy, J. C.; Murthy, N.; Sulchek, T. A.; Barker, T. H.; García, A. J. Maleimide Cross-Linked Bioactive PEG Hydrogel Exhibits Improved Reaction Kinetics and Cross-Linking for Cell Encapsulation and in Situ Delivery. *Adv. Mater.* **2012**, *24* (1), 64–70.
- (44) Stohs, S. J. The Role of Free Radicals in Toxicity and Disease. *J. Basic Clin. Physiol. Pharmacol.* **1995**, *6* (3–4), 205–228.
- (45) Bryant, S. J.; Nuttelman, C. R.; Anseth, K. S. Cytocompatibility of UV and Visible Light Photoinitiating Systems on Cultured NIH/3T3 Fibroblasts in Vitro. *J. Biomater. Sci. Polym. Ed.* **2000**, *11* (5), 439–457.
- (46) Sun, J. Y.; Zhao, X.; Illeperuma, W. R. K.; Chaudhuri, O.; Oh, K. H.; Mooney, D. J.; Vlassak, J. J.; Suo, Z. Highly Stretchable and Tough Hydrogels. *Nature* **2012**, *489* (7414), 133–136.
- (47) Sultan, S.; Siqueira, G.; Zimmermann, T.; Mathew, A. P. 3D Printing of Nano-Cellulosic Biomaterials for Medical Applications. *Curr. Opin. Biomed. Eng.* **2017**, *2*, 29–34.
- (48) Leppiniemi, J.; Lahtinen, P.; Paajanen, A.; Mahlberg, R.; Metsä-Kortelainen, S.; Pinomaa, T.; Pajari, H.; Vikholm-Lundin, I.; Pursula, P.; Hytönen, V. P. 3D-Printable Bioactivated Nanocellulose–Alginate Hydrogels. *ACS Appl. Mater. Interfaces* **2017**, *9* (26), 21959–

21970.

- (49) Broguiere, N.; Formica, F.; Barreto, G.; Zenobi-Wong, M. Sortase A as a Cross-Linking Enzyme in Tissue Engineering. *Acta Biomater.* **2018**, No. July.
- (50) Vercreyusse, K. P.; Marecak, D. M.; Marecek, J. F.; Prestwich, G. D. Synthesis and in Vitro Degradation of New Polyvalent Hydrazide Cross-Linked Hydrogels of Hyaluronic Acid. *Bioconjug. Chem.* **1997**, *8* (5), 686–694.
- (51) Bouten, P. J. M.; Hertsen, D.; Vergaelen, M.; Monnery, B. D.; Boerman, M. A.; Goossens, H.; Catak, S.; van Hest, J. C. M.; Van Speybroeck, V.; Hoogenboom, R. Accelerated Living Cationic Ring-Opening Polymerization of a Methyl Ester Functionalized 2-Oxazoline Monomer. *Polym. Chem.* **2015**, *6* (4), 514–518.
- (52) Arkenberg, M. R.; Moore, D. M.; Lin, C. C. Dynamic Control of Hydrogel Crosslinking via Sortase-Mediated Reversible Transpeptidation. *Acta Biomater.* **2019**, *83*, 83–95.
- (53) Williamson, D. J.; Fascione, M. A.; Webb, M. E.; Turnbull, W. B. Efficient N-Terminal Labeling of Proteins by Use of Sortase. *Angew. Chemie Int. Ed.* **2012**, *51* (37), 9377–9380.
- (54) Chaudhuri, O.; Gu, L.; Klumpers, D.; Darnell, M.; Bencherif, S. A.; Weaver, J. C.; Huebsch, N.; Lee, H.; Lippens, E.; Duda, G. N.; et al. Hydrogels with Tunable Stress Relaxation Regulate Stem Cell Fate and Activity. *Nat. Mater.* **2016**, *15* (3), 326–334.
- (55) Huang, M.; Furukawa, H.; Tanaka, Y.; Nakajima, T.; Osada, Y.; Gong, J. P. Importance of Entanglement between First and Second Components in High-Strength Double Network Gels. *Macromolecules* **2007**, *40* (18), 6658–6664.
- (56) Groll, J.; Boland, T.; Blunk, T.; Burdick, J. A.; Cho, D.-W.; Dalton, P. D.; Derby, B.;

- Forgacs, G.; Li, Q.; Mironov, V. A.; et al. Biofabrication: Reappraising the Definition of an Evolving Field. *Biofabrication* **2016**, *8* (1), 13001.
- (57) Ozbolat, I. T.; Hospodiuk, M. Current Advances and Future Perspectives in Extrusion-Based Bioprinting. *Biomaterials* **2016**, *76*, 321–343.
- (58) Moroni, L.; Boland, T.; Burdick, J. A.; Maria, C. De; Derby, B.; Forgacs, G.; Groll, J.; Li, Q.; Malda, J.; Mironov, V. A.; et al. Biofabrication: A Guide to Technology and Terminology. *Trends Biotechnol.* **2018**, *36* (4), 384–402.
- (59) Figueiredo, L.; Pace, R.; D’Arros, C.; Réthoré, G.; Guicheux, J.; Le Visage, C.; Weiss, P. Assessing Glucose and Oxygen Diffusion in Hydrogels for the Rational Design of 3D Stem Cell Scaffolds in Regenerative Medicine. *J. Tissue Eng. Regen. Med.* **2018**, *12* (5), 1238–1246.
- (60) Malda, J.; Visser, J.; Melchels, F. P.; Jüngst, T.; Hennink, W. E.; Dhert, W. J. A.; Groll, J.; Hutmacher, D. W. 25th Anniversary Article: Engineering Hydrogels for Biofabrication. *Adv. Mater.* **2013**, *25* (36), 5011–5028.
- (61) Chang, R.; Nam, J.; Sun, W. Effects of Dispensing Pressure and Nozzle Diameter on Cell Survival from Solid Freeform Fabrication–Based Direct Cell Writing. *Tissue Eng. Part A* **2008**, *14* (1), 41–48.
- (62) Schenk, V.; Rossegger, E.; Ebner, C.; Bangerl, F.; Reichmann, K.; Hoffmann, B.; Höpfner, M.; Wiesbrock, F. RGD-Functionalization of Poly(2-Oxazoline)-Based Networks for Enhanced Adhesion to Cancer Cells. *Polymers (Basel)*. **2014**, *6* (1), 264–279.
- (63) Lorson, T.; Jaksch, S.; Lübtow, M. M.; Jüngst, T.; Groll, J.; Lühmann, T.; Luxenhofer, R.

A Thermogelling Supramolecular Hydrogel with Sponge-Like Morphology as a Cytocompatible Bioink. *Biomacromolecules* **2017**, *18* (7), 2161–2171.

- (64) Blöhbaum, J.; Paulus, I.; Pöppler, A.-C.; Tessmar, J.; Groll, J. Influence of Charged Groups on the Cross-Linking Efficiency and Release of Guest Molecules from Thiol–Ene Cross-Linked Poly(2-Oxazoline) Hydrogels. *J. Mater. Chem. B* **2019**, *7* (10), 1782–1794.